

High-Performance of Nanoparticles and Their Effects on The Mechanical, Thermal Stability and UV-Shielding Properties of PMMA Nanocomposites

Hesham Moustafa^{1*}, Nabila A. Darwish¹, Ahmed M.Youssef³, Sameh M. Reda², Abd El-Aziz A. El-Wakil¹

¹Polymer Metrology & Technology Department, National Institute of Standards (NIS), Tersa Street, El Haram, El-Giza, P.O Box 136, Giza 12211, Egypt.

²Photometry and Radiometry Department, National Institute of Standards (NIS), Tersa Street, El Haram, El-Giza, P.O Box 136, Giza 12211, Egypt.

³Packing and Packaging Materials Department, National Research Centre, 33 El Bohouth St. (former El Tahrir st.), Dokki, Giza, Egypt, P.O. 12622

THE TARGET of this work is to choose a suitable nanoparticle for preparing a highly ultraviolet (UV)-shielding from poly (methylmethacrylate) (PMMA) nanocomposites at low concentration and to decrease the destructive effects of UV radiation. Morphologies of the synthesized nanoparticles were investigated by X-ray diffraction (XRD), scanning and transmission electron microscopy (SEM and TEM). Whereas, pure PMMA and its nanocomposites were characterized by using dynamic mechanical analysis (DMA), tensile testing, UV-visible spectra (T%), and thermogravimetric analysis (TGA). The obtained results showed a good correlation between the tensile properties, DMA and TGA analysis depending on the type of nanoparticles used in the PMMA matrix, especially in case of ZrO₂ and ZnO. Furthermore, UV-vis spectra were analyzed ranging from 200 nm to 800 nm. It showed that UV radiation is significantly blocked from 100% to 0.2 % in the UV range between 200 nm and 360 nm for pure PMMA and to 0.08 % for PMMA/CeO₂ nanocomposite and to 0.01 % for PMMA/CeO₂ with various types of nanoparticles. After 360 nm, pure PMMA and PMMA/CeO₂ were a little bit affected by UV lights, whereas the PMMA based on different nanoparticles was not affected. This result demonstrates that these nanocomposites could be strongly candidates for the sunscreens or for several fields that related to the UV photodegradation effects.

Keywords: Nanoparticles, PMMA nanocomposites, X-ray diffraction, UV-visible spectra, tensile properties, Thermogravimetric analysis.

Introduction

Recently, many studies have confirmed that ultraviolet (UV) radiations become harmful for human health, especially after the thinning of the ozone layer, which caused severely negative effects on the human eyes. They also damage the DNA molecules in the skin cells and which lead to a skin cancer, as well as other effects such as immune system [1-5]. In addition, UV radiations have degradation effects on many materials such as textile's dye, polymers, medical and semiconductor equipment [6,7]. Therefore, great research efforts have been dedicated to developing the UV shielding materials which could be used in the UV blocking applications such as sunscreens,

UV protecting coatings, optical filters, etc [8-12].

Several researches have been done on the poly (methyl methacrylate) (PMMA) as a thermoplastic material for UV-protection due to its transparency in the visible region. Nevertheless, its application is limited not only at higher temperature due to its poor thermal stability, but also due to its relatively resistant for UV light. The combination of PMMA matrix with inorganic materials (i.e, metal oxides) such as CeO₂[13], TiO₂[14,15], ZrO₂[16,17], ZnO[18,19] and silica [20], are resulting in new and often unique properties. Among of them, the thermal stability and optical properties in the UV-rays region are improved. Nowadays, the metal

*Corresponding author e-mail: hesham.moustafa21@gmail.com; Tel: +201 0173 4580 0; Fax: 0020 2338 6745 1
DOI:10.21608/ejchem.2017.1932.1159

oxides in nanoscales, especially with PMMA polymer exhibit an excellent candidate for flame retardance, electrical behavior, antimicrobial activity and UV-blocking. This is due to their ability to interact with the functional groups in the backbone polymer matrices as well as their high resistivity to decompose at elevated temperature. A few researches have explored the blending of silica, ZnO or CaCO₃ nanoparticles with polystyrene matrix, to enhance its properties, particularly UV-protecting ability based on transparent nanocomposite films [21,22]. However, studies on the combination of PMMA/CeO₂ with different types of nanoparticles such as silica, Ag doped TiO₂ NPs, ZrO₂, and ZnO by using melt blending method have seldom been reported. The CeO₂ nanoparticles have excellent UV absorption property as compared to ZnO, TiO₂ and ZrO₂. However, one of the drawbacks of CeO₂ particles is liable to aggregate in the polymer matrix because of their high surface energy and activity. For this reason, the introduction of another nanoparticle with CeO₂ into the same matrix is essential to avoid its aggregation in the polymer matrix and thereby improve its properties. Therefore, in this research, we attempted to prepare PMMA nanocomposites, based on different nanoparticles at low contents, with high durability against UV photodegradation. The effect of the introduction of various types of nanocomposites on the mechanical, dynamic, thermal stability and UV-shielding properties was investigated.

Experimental

Materials

Titanium (IV) isopropoxide (TTIP) and Silver nitrate (AgNO₃) were obtained from Sigma-Aldrich, Egypt. Zinc-acetate (puriss, Reanal, Hungary) (Zn (CH₃COO)₂·2H₂O) was used to prepare ZnO nanoparticle. Commercial poly (methyl methacrylate) (PMMA) was offered from CHI MEI Corporation, Taiwan. Cerium Oxide (CeO₂) (< 25 nm) and Zirconium oxide (ZrO₂) nanopowders (particle size < 100 nm) were purchased from Sigma-Aldrich, Egypt. The silica nanopowder (primary particle size 12 nm measured by TEM) with assay 99.8% was purchased from Sigma-Aldrich, Egypt. Other reagents which used in synthesis of ZnO and TiO₂ and Ag doped in TiO₂ were obtained from Merck, Germany.

Preparation of TiO₂ nanoparticles (TiO₂-NPs)

In classic method TiO₂-NPs was prepared using TTIP as a precursor and was mixed with

HCl, ethanol and de-ionized water mixture, stirred for 2 h, in pH at 1.5. Then 10 ml of de-ionized water was added to the above mixture and stirred for another 2 h at room temperature. Finally, the solution was dried in electrical oven and the powder was heated at 120°C for 1 h.

Synthesis of TiO₂ nanoparticles doped silver (Ag-TiO₂ NPs)

Ag-NPs doped TiO₂ nanoparticles were prepared through photo-reducing Ag⁺ ions to Ag metal on the TiO₂ nanoparticle surface via the following method [23]. First pH of the TiO₂ nanoparticle suspension was adjusted to 3.5 taking place to reaction using perchloric acid. Aliquots of different amounts of Ag⁺ ions, set by dissolving silver nitrate salt (AgNO₃) in deionized water, were added into the suspension of TiO₂ nanoparticles such that the Ag⁺ concentration was 5% in relation to TiO₂ nanoparticles. The mixtures were then exposed to irradiation using UV light by four mercury lamps (8 W) for 6 h with constant air stream. The suspensions were then filtered, washed and dried to give Ag doped TiO₂ nanoparticles.

Preparation of ZnO Nanoparticles

In order to prepare ZnO-NPs, standard solution of Zn(CH₃COO)₂·2H₂O (0.2 M) was prepared in 50 mL methanol with stirring. To this stock solution 50 mL of NaOH (0.5M) in methanol was added with continuous stirring in order to reach the pH value of reactants between 8 and 11. The solution was transferred into Teflon lined sealed stainless steel autoclaves and stored at various temperatures in the range of 100 to 200°C for 6 and 12 h under autogenous pressure. It was then allowed to cool naturally to room temperature. After the reaction was completed, the resulting white solid product was washed with methanol, filtered and then dried in a laboratory oven at 60°C for 12h.

Melt blending of PMMA and its nanocomposites

The nanocomposites PMMA, CeO₂ and nanoparticles with fixed 2 wt. % content for each one were prepared by melt blending method at 200°C in Brabender Plasti-Corder, USA with a speed rate 80 rpm for 15 min for each specimen. Where, the polymer and stearic acid were firstly added into the mixing chamber for 3 min and then 2 wt. % of CeO₂ introduced to the mix, followed by 2 wt. % of each nanoparticle for a total mixing time of 15 min. Composition and codification of the investigated specimens are shown in Table 1.

Characterization Methods

Morphology of synthesized nano-particles

The morphology of the synthesized nano-particles was characterized by transmission electron microscopy (TEM), scanning electron microscopy (SEM) and X-ray diffraction (XRD) techniques. The XRD patterns investigations of the prepared nanomaterials were carried out on a Diano X-ray diffractometer using $\text{CoK}\alpha$

radiation source energized at 45 kV and a Philips X-ray diffractometer (PW 1930 generator, PW 1820 goniometer) with CuK radiation source ($\lambda=0.15418$ nm). The basal spacing (dL) was calculated from the (001) reflection via the Bragg's equation. The surface morphology of prepared nanomaterials were analyzed using scanning electron microscopy (SEM), (JSM 6360LV, JEOL/Noran). The nanostructure of the prepared

TABLE 1. Formulations and tensile properties of pure PMMA and its nanocomposites.

Ingredients, wt. %	Pure PMMA	PMMA/CeO ₂	PMMA/silica	PMMA/Ag-TiO ₂ NPs	PMMA/ZrO ₂	PMMA/ZnO
PMMA	100	98	96	96	96	96
Stearic acid	3	3	3	3	3	3
CeO ₂	-	2	2	2	2	2
Nano-silica	-	-	2	-	-	-
Ag-TiO ₂ NPs	-	-	-	2	-	-
Nano-ZrO ₂	-	-	-	-	2	-
Nano-ZnO	-	-	-	-	-	2
Tensile strength at max., (MPa)	30.6±0.34	31.2±0.47	32.1±0.40	33.7±0.64	45.2±0.53	48.4±0.45
Elongation at break, %	6.9±1.20	7.5±1.62	7.9±1.33	8.2±1.45	8.9±1.82	10.7±1.30

nanomaterials was elucidated by JEOL JEM-1230 transmission electron microscope (TEM) with acceleration voltage of 80 kV. The microscopy probes of the nanomaterials was prepared by adding a small drop of the water dispersions onto a Lacey carbon film-coated copper grid then allowing them to dry in air.

Dynamic mechanical analysis (DMA)

The DMA analysis was conducted on TA Instruments (Model Q800, TA Instruments, USA) from 30 °C to 170 °C at a heating rate of 5 K/min, and at a frequency of 1 Hz in the tension mode and with a % strain of 0.02. Sample size was 30 × 6 × 2 mm³.

Mechanical properties

The tensile properties of pure PMMA and its nanocomposites were determined on sheets of dimensions 100 × 100 × 2 mm³. Type 2 dumbbell test samples were die-cut from the molded sheets. The tensile strength at maximum and elongation at break were determined using a Zwick (Germany) tensile testing machine (Model Z010), at a temperature of 23 ± 2 °C and a crosshead speed of 5 mm/min according to ASTM D 638. The standard uncertainty was calculated from four measurements for each sample.

UV-visible spectra

The UV-visible transmittance spectra of the pure PMMA and its nanocomposites was conducted

using a Hamamatsu mini spectrometer model C10082CAH with CCD of spectral response 200-800 nm image sensor. The transmittance (T%) was calculated using equation 1 as follows:

$$T \% = \left(\frac{I}{I_0} \right) * 100 \quad (1)$$

Where: I_0 is the intensity of the deuterium lamp passing through air,

I is the intensity of the same lamp passing through each sample.

The uncertainty value for transmittance was calculated for ten measurements of each sample. The setup shown in Fig.1 for measuring the transmittance consists of mini spectrometer mentioned before, sample holder, UV-Visible source, and computer with a program to collect the output data.

Thermogravimetric analysis (TGA)

The TGA analysis for pure PMMA and its filled nanocomposites was carried out on the TGA-50 (Shimadzu Thermogravimetric analyzer, Japan) using a heating rate of 10 °C/min in a nitrogen atmosphere.

Results and Discussion

Morphology of the nanoparticles

The morphology of the synthesized

nanoparticles was characterized by transmission electron microscopy (TEM), scanning electron microscopy (SEM) and X-ray diffraction (XRD) techniques. The Ag-TiO₂-NPs nanocomposites were demonstrated using XRD to determine the phase structure of the samples. Figure 2a displays the XRD pattern of TiO₂ nanoparticles doped by Ag-NPs, the pattern can be assigned to the diffraction of (111), (200), (220), and (311) planes of face centered cubic (fcc) Ag-NPs, which are noticeable with Ag in Fig. 2a. Correspondingly, this pattern establishes that additional peaks appear, which can be ascribed to the anatase phase

of TiO₂ signifying that the formation of TiO₂-Ag-NPs nanocomposites, and this is correlated with SEM and TEM observations. Moreover, the TEM studies were carried out to examine the surface morphology of information on the TiO₂-Ag-NPs nanocomposites. The common morphology of the TiO₂ nanoparticles doped Ag is detected in Fig.2b. It is clear that the main particles have diameters <15 nm, small weak agglomerates are fashioned that rise with increasing Ag content. Correspondingly, the SEM image of TiO₂-NPs and Ag doped TiO₂-Ag-NPs nanocomposites are as well revealed in Figure2c. It shows that the

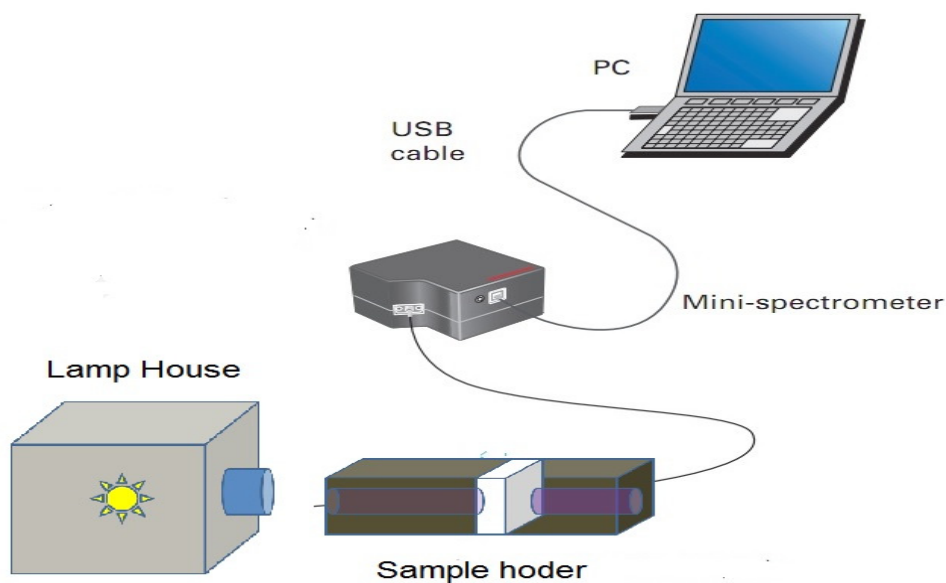


Fig. 1. Schematic diagram of transmittance measuring setup.

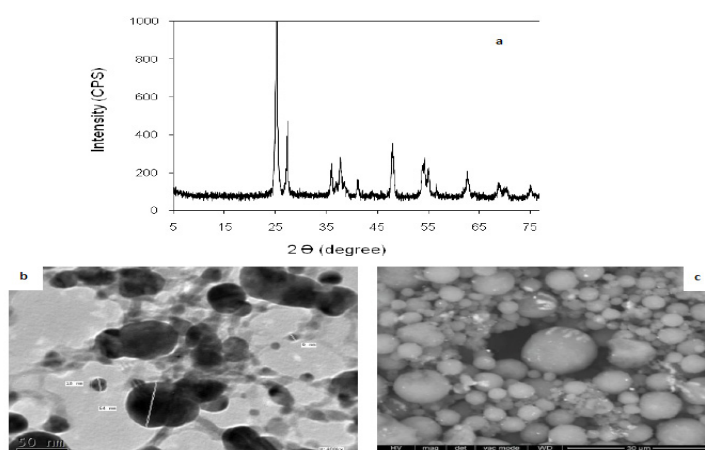


Fig. 2.(a) XRD and (b) TEM and (c) SEM images for Ag-TiO₂ NPs.

dispersion of Ag-NPs on the surface of TiO_2 -NPs which is uniform and comprises unequal designed particles which are the accumulation of small crystals.

XRD patterns of the prepared ZnO-NPs were plotted in Figure 3d. The data were collected using 2θ range from 10° to 80° and completely the characteristic peaks of ZnO-NPs appear (100) at

$2\theta = 31.8^\circ$, (002) appear at $2\theta = 34.4^\circ$, (101) at $2\theta = 36^\circ$, (102) at 2θ of 47° , (110) at $2\theta = 56^\circ$, (103) seems at $2\theta = 62^\circ$ and (112) fall at $2\theta = 68^\circ$. These peaks confirm that high purity of ZnO nanoparticles is synthesized. Furthermore, XRD diffraction pattern displays that the preparation of ZnO nanoparticles with quartzite phase and all the diffraction peaks fixed with the reported JCPDS data (no characteristic peaks are observed other

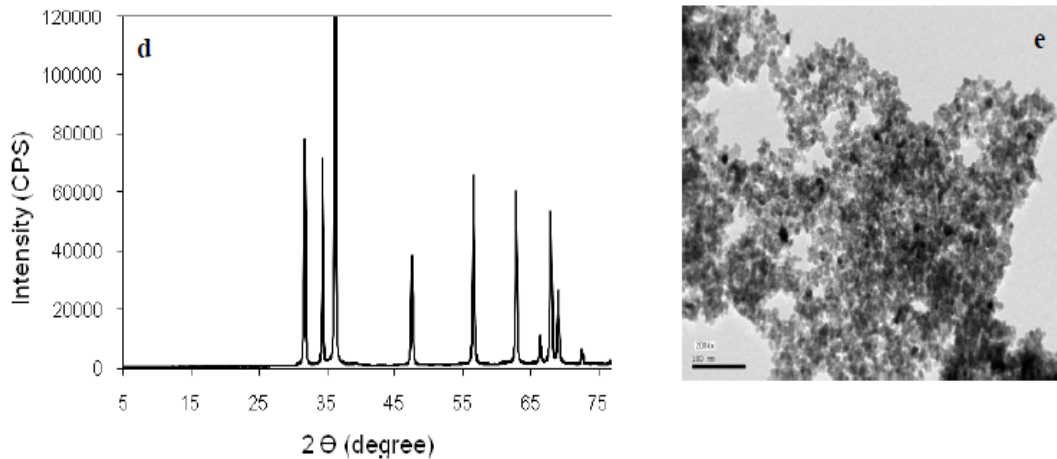


Fig. 3. (d) XRD patterns and (e) TEM images for ZnO-NPs.

than ZnO and the ZnO nanoparticles) is established using TEM, in which ZnO nanoparticles appear as spherical shape with particle size around 5–9 nm as shown in (Figure 3e).

Dynamic mechanical analysis

Figure 4 (a and b) shows the storage modulus (E') and the damping, $\tan \delta$ obtained as a function of temperature for pure PMMA and its nanocomposites at various types of nanoparticles. As shown in the figure, there is no effect on the E' and $\tan \delta$ with the introduction of 2 wt.% of CeO_2 content as compared to pure PMMA. Upon the addition of 2 wt.% nanoparticles, the E' values at the glassy region significantly increase in the following order: silica \leq Ag- TiO_2 NPs $<$ ZrO_2 $<$ ZnO, demonstrating the reinforcing effect of these nanoparticles and the competition of their chemical reactions with the investigated polymer. Moreover, in Figure 4b, the $\tan \delta$ and the glass transition temperature (T_g) values are gradually shifted to higher temperature in the same order from 134°C to 145°C as compared to pure PMMA and PMMA/ CeO_2 nanocomposite. This shift in T_g values is apparently ascribed to the restrictions of the polymer chain mobility, which might be caused by the presence of new crosslinking networks

formed either via the chemical bonds or the hydrogen bonding or both with the addition of those nanoparticles [16,24,25], particularly in case of ZrO_2 and ZnO.

Mechanical properties

The tensile properties, as tensile strength at maximum and elongation at break for pure PMMA and its nanocomposites with various types of nanofillers, have been determined and the results are summarized in Table 1. The tensile strength of pure PMMA is 30.6 MPa, but its value increased a little bit to 31.2 MPa on adding 2 wt.% of CeO_2 filler. Upon the addition of 2 wt.% of different nanoparticles into PMMA, the tensile values of PMMA nanocomposites are increased to 32.1 MPa, 33.7 MPa, 45.2 MPa, and 48.4 MPa for PMMA/silica, PMMA/Ag- TiO_2 NPs, PMMA/ ZrO_2 , and PMMA/ZnO, respectively. The enhancement in the tensile strength may be due to the formation of crosslinking networks after introducing these nanoparticles, especially in case of ZrO_2 and ZnO, in addition to the hydrogen bonding interaction between the stearic acid in the polymer matrix and the nanoparticles. This fact illustrates the better interaction between PMMA matrix and these two nanofillers. The

correlation between the tensile values (static test) and DMA data (dynamic test), which are presented above, is observed in terms of the effect of type of nanoparticle on the polymer matrix

[26]. On the other hand, the elongation at break is increased from 7.5% for CeO_2 to 10.7% for ZnO as compared to unfilled PMMA (6.9%), as shown in Table 1. This increase is probably due

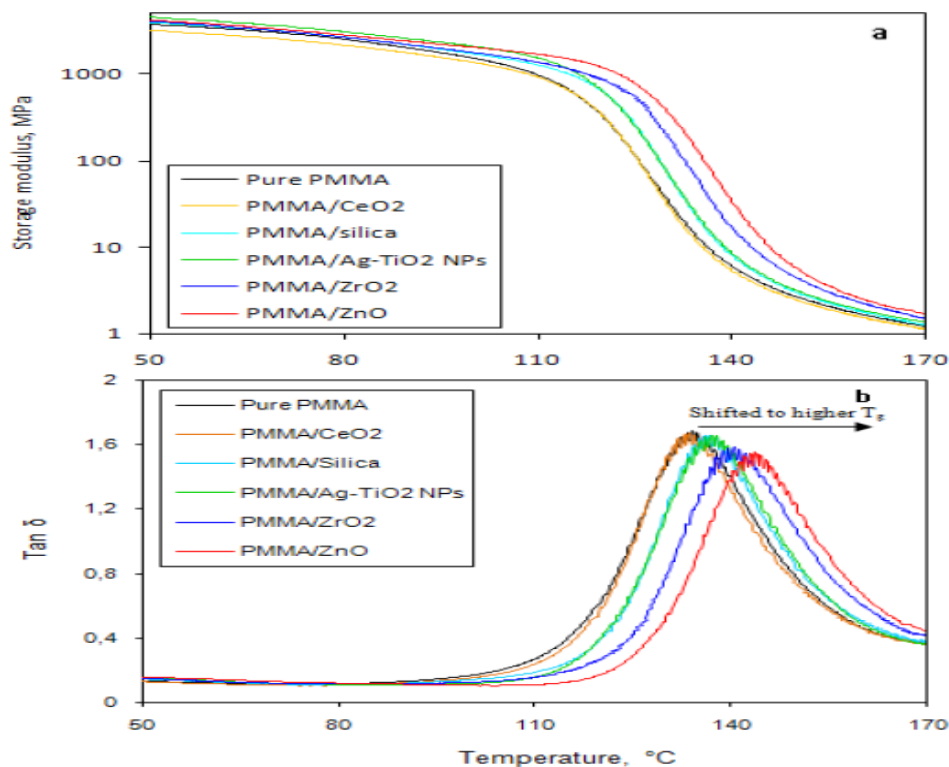


Fig. 4. Storage modulus (a) and $\tan \delta$ (b) of pure PMMA and its nanocomposites with different types of nano-fillers.

to the hydrogen bonding formed which can be easily broken under high strength and renders the nanocomposite more ductile rather than the pure polymer [16].

UV-visible spectra

The UV-visible transmittance spectra ($T\%$) of the pure PMMA and its nanocomposites at various types of nanoparticles from 200 nm to 800 nm, is shown in Figure 5. The study of $T\%$ is divided into three parts to show the effect of nanoparticles on the UV-shielding at lower filler content: the first one is done for pure PMMA, the second for PMMA/ CeO_2 (2 wt. %) nanocomposite, and the third one for PMMA/ CeO_2 with different types of nanoparticles as seen in Table 1. Figure 5 shows that for pure PMMA, UV radiation is blocked from 100% to 0.2% in the UV range between 200 nm and 360 nm and for PMMA/ CeO_2 nanocomposite to 0.08% and for PMMA/ CeO_2 with various types of nanoparticles to 0.01%. Correspondingly, Aklalouch *et al.* [27] have been reported that PMMA/30% CeO_2 nanocomposite

provided a good UV-protection, while pure PMMA or PMMA/2% CeO_2 nanocomposite showed an excellent UV-shielding in our case, this may be due to the presence of stearic acid in the matrix which plays a significant role in UV-inhibition. Whereas, the effect of UV radiation increases after 360 nm in case of pure PMMA and its nanocomposite based on CeO_2 , this may be due to the photodegradation of the PMMA matrix [28-2930]. However, the peaks of polymer based on different types of nanoparticles seem remaining in prolong of UV range, as shown in Figure 5. This confirms the strong chemical interaction, i.e., crosslinking network formations between the polymer and these nanocomposites occurred, and aren't affected by UV lights. On the other hand, the visible light is also affected gradually by pure PMMA and its nanocomposites because of their translucidity, as shown in Fig. 5. Therefore, it can be said that all UV light are blocked with these nanocomposites and with long period but unfortunately it affects the optical transparency.

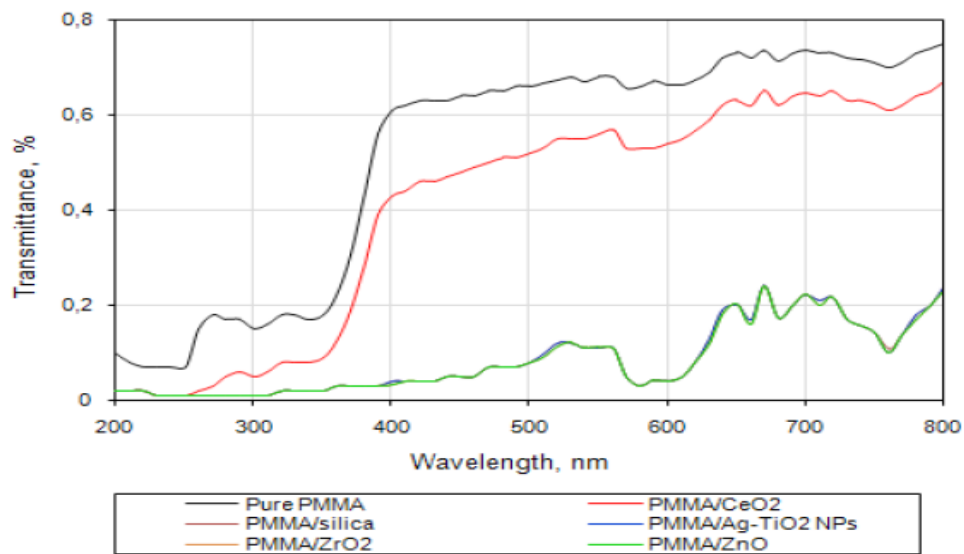


Fig. 5. UV-vis spectra of pure PMMA and its nanocomposites slabs with different types of nano-fillers (thickness of slabs: 1.0 mm).

Thus, these nanocomposites could strongly be considered candidates in the sunscreens and in the medical equipment.

Thermogravimetric analysis (TGA)

TGA curves of all the investigated nanocomposites under nitrogen atmosphere are shown in Fig. 6. The pure PMMA shows one step in which it degrades around 350°C and without remaining residue. On addition of 2 wt.% CeO₂ filler content, the thermal stability of PMMA

improved by 9°C at the temperature steadily ($T_{0.5}$, designated as 50 wt.% weight loss) as compared to pure polymer. Upon addition of 2 wt. % of different types of the nanoparticles to the PMMA/CeO₂ nanocomposite, $T_{0.5}$ increases to 363°C, 366°C, 367°C, and 368°C with adding silica, Ag-TiO₂ NPs, ZrO₂, and ZnO nanoparticles, respectively, indicating an enhancement of the thermal stability of PMMA nanocomposites. This enhancement in the thermal stability may be due to the formation of networks (i.e., via the

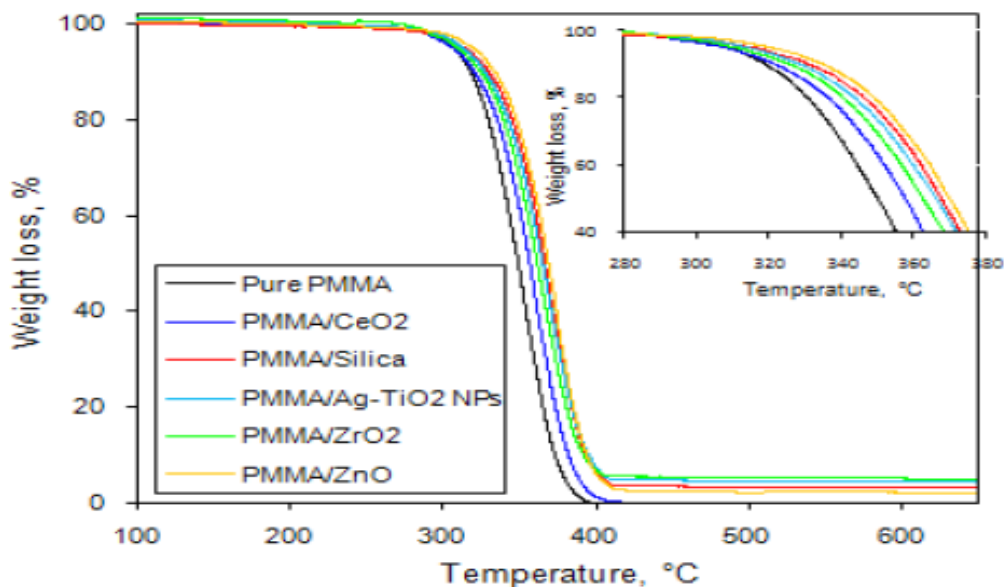


Fig. 6. TGA curves of pure PMMA and its nanocomposites with different types of nano-fillers in N₂ atmosphere.

chemical bonds) between the PMMA polymer and these inorganic moieties, which retard the thermal degradation of PMMA matrix at high temperature.

Conclusion

The purpose of the present work is to investigate the effect of different nanoparticles on UV-shielding properties of PMMA nanocomposite:

1. The nanocomposites of PMMA with various nanoparticles are prepared using the melt compounding method.
2. Characterization of the studied nanoparticles by TEM, SEM and XRD has revealed that Ag-NPs are dispersed on the surface of TiO₂-NPs which is uniform and comprises unequal designed particles.
3. The presence of Ag-NPs is confirmed by XRD technique. On the other hand, XRD patterns of the prepared ZnO-NPs has pointed out that high purity of ZnO nanoparticles are synthesized. This is also confirmed by TEM.
4. DMA results show a significant enhancement in the storage modulus in the glassy region and T_g values are shifted to higher temperature by adding 2 wt% of nanoparticles, particularly in case of ZrO₂ and ZnO, to PMMA.
5. The tensile strength and the thermal stability properties are improved when different types of nanoparticles, especially ZrO₂ and ZnO, are used. On the other hand, the elongation at break is increased with the addition of these nanoparticles. This increase may be due to the formation of hydrogen bonding which can be easily broken and renders the nanocomposite more ductile rather than pure polymer.
6. An excellent UV-shielding is obtained when PMMA/CeO₂ with different types of nanoparticles, which could be used in variety applications such as sunscreens, aerospace, and several fields that related to the UV photodegradation effects.

References

1. Ries G., Heller W., Puchta H., Sandermann H., Seidlitz H.K. and Hohn B., Elevated UV-B radiation reduces genome stability in plants. *Nature* **406**, 98-101(2000).
2. De Gruijl F.R., Longstreth J., Norval M., Cullen A.P., Slaper H., Kripke M.L., Takizawa

Y. and Van der Leun J.C. Health effects from stratospheric ozone depletion and interactions with climate change. *Photochem. Photobiol. Sci.* **2**, 16-28 (2003).

3. Wang L.E., Li C.Y., Strom S. S., Goldberg L.H., Brewster A, Guo Z .Z., Qiao Y. W., Clayman G. L., Lee J. J., El-Naggar A.K., Prieto V.G., Duvic M., Lippman S.M., Weber R.S., Kripke M.L. and Wei Q.Y., Repair capacity for UV light-induced DNA damage associated with risk of nonmelanoma skin cancer and tumor progression. *Clin. Cancer Res.* **13**, 6532-6539 (2007).
4. Li S., Toprak M.S., Suk Jo Y., Dobson J., Kim D.K. and Muhammed M., Bulk synthesis of transparent and homogeneous polymeric hybrid materials with ZnO quantum dots and PMMA. *Adv. Mater.* **19**, 4347-4352 (2007).
5. Eita M., Wagberg L. and Muhammed M., Spin-assisted multilayers of poly(methyl methacrylate) and zinc oxide quantum dots for ultraviolet-blocking applications. *ACS Appl. Mater. Interfaces* **4**, 2920-2925 (2012).
6. Pardo R., Zayat M. and Levy D., Effect of the chemical environment on the light-induced degradation of a photochromic dye in ormosil thin films. *J. Photochem. Photobiol. A*, **198**, 232-236 (2008).
7. Perotti M.G. and Dieguez M.D.C., Effect of UV-B exposure on eggs and embryos of Patagonian anurans and evidence of photoprotection. *Chemosphere* **65**, 2063-2070 (2006).
8. Wang J. X., Liang J., Wu H.M., Yuan W.F., Wen Y.Q., Song Y.L. and Jiang L., A facile method of shielding from UV damage by polymer photonic crystals. *Polym. Int.* **57**, 509-514 (2008).
9. Sun D., Sue H.J. and Miyatake N., Optical properties of ZnO quantum dots in epoxy with controlled dispersion. *J. Phys. Chem. C* **112**, 16002-16010 (2008).
10. Yabe S., Yamashita M., Momose S., Tahira K., Yoshida S., Li R., Yin S. and Sato T., Preparation and UV-shielding properties of silica-coated ceria nanocomposite. *Int. J. Inorg. Mater.* **3**, 1003-1008 (2001).
11. Mazzocchetti L., Cortecchia E. and Scandola M., Organic-inorganic hybrids as transparent

- coatings for uv and X-ray shielding. *ACS Appl. Mater. Interfaces* **1**, 726-734 (2009).
12. Wu P-S., Huang L-N., Guo Y-C. and Lin C-C., Effects of the novel poly(methyl methacrylate) (PMMA)-encapsulated organic ultraviolet (UV) filters on the UV absorbance and in vitro sun protection factor (SPF). *J. Photochem. Photobiol.* **B131**, 24-30 (2014).
 13. Caia G., Xub S., Wangb Z. and Wilkie C.A., Further studies on polystyrene/cerium (IV) oxide system: melt blending and interaction with montmorillonite. *Polym. Adv. Technol.* **25**, 217-222 (2014).
 14. Yuwono A.H., Xue J., Wang J., Elim H.I., Ji W., Li Y. and White T.J., Transparent nanohybrids of nanocrystalline TiO₂ in PMMA with unique nonlinear optical behavior. *J. Mater. Chem.* **13**, 1475-1479 (2003).
 15. El-Wakil A. A., Moustafa H. and Helaly F. M., Utilization of nano-powder barium strontium titanium oxide ((BaTiO₃)(SrTiO₃)) for improving the properties of acrylonitrile butadiene rubber. *Res. J. Pharm. Biol. Chem. Sci.* **6**, 1150-1162 (2015).
 16. Hu Y., Gu G., Zhou S. and Wu L., Preparation and properties of transparent PMMA/ZrO₂ nanocomposites using 2-hydroxyethyl methacrylate as a coupling agent. *Polymer* **52**, 122-129(2011).
 17. Maji P., Choudhary R.B. and Majhi M., Structural, optical and dielectric properties of ZrO₂ reinforced polymeric nanocomposite films of polymethylmethacrylate (PMMA). *Optik.* **127**, 4848-4853 (2016).
 18. Podbrscek P., Drazic G., Anzlovar A. and Orel Z.C. The preparation of zinc silicate/ZnO particles and their use as an efficient UV absorber. *Mater. Res. Bull.* **46**, 2105-2111 (2011).
 19. Zhang Y., Zhuang S., Xu X., and Hu J. Transparent and UV-shielding ZnO@PMMA nanocomposite films. *Opt. Mater.* **36**, 169-172 (2013).
 20. Wang H., Xu P., Meng S., Zhong W., Du W. and Du, Q., Poly(methyl methacrylate)/silica/titania ternary nanocomposites with greatly improved thermal and ultraviolet-shielding properties. *Polym. Degrad. Stab.* **91**, 1455-1461 (2006).
 21. Wu T., and Ke Y., Melting, crystallization and optical behaviors of poly (ethylene terephthalate) silica/ polystyrene nanocomposite films. *Thin Solid Films* **515**, 5220-5226 (2007).
 22. Pal M.K., Singh B. and Gautam J., Thermal stability and UV-shielding properties of polymethyl methacrylate and polystyrene modified with calcium carbonate nanoparticles. *J. Therm. Anal. Calorim.* **107**, 85-96 (2012).
 23. Hebeisha A., Abdelhadya M.M. and Youssef A.M., TiO₂ nanowire and TiO₂ nanowire doped Ag-PVP nanocomposite for antimicrobial and self-cleaning cotton textile. *Carbohydr. Polym.* **91**, 549-559 (2013).
 24. Moustafa H., Youssef A.M., Duquesne S. and Darwish N.A., Characterization of bio-filler derived from seashell wastes and its effect on the mechanical, thermal, and flame retardant properties of ABS composites. *Polym. Compos.* (2015) DOI 10.1002/pc.23878 (in press).
 25. Moustafa H. and Darwish N.A., Effect of different types and loadings of modified nanoclayon mechanical properties and adhesion strength of EPDM-g-MAH/nylon 66 systems. *Int. J. Adhes. Adhes.* **61**, 15-22 (2015).
 26. Bosze E.J., Alawar A., Bertschger O., Tsai Y-I. and Nutt S.R., High-temperature strength and storage modulus in unidirectional hybrid composites. *Compos. Sci. Technol.* **66**, 1963-1969 (2006).
 27. Aklalouch M., Calleja A., Granados X., Ricart S., Boffa V., Ricci F., Puig T. and Obradors X., Hybrid sol-gel layers containing CeO₂ nanoparticles as UV-protection of plastic lenses for concentrated photovoltaics. *Sol. Energ. Mat. Sol. Cells* **120**, 175-182 (2014).
 28. Zayat M., Garcia-Parejo P. and Levy D., Preventing UV-light damage of light sensitive materials using a highly protective UV-absorbing coating. *Chem. Soc. Rev.* **36**, 1270-1281 (2007).
 29. Ranby B.G. and Rabek J.F., *Photodegradation, Photo-Oxidation, and Photostabilization of Polymers: Principles and Applications*, John Wiley & Sons (1975).

30. Bennet F., Hart-Smith G., Gruending T., Davis T.P., Barker P.J. and Barner-Kowollik C., Degradation of poly (methyl methacrylate) model compounds under extreme environ-

mental conditions. *Macromol. Chem. Phys.* **211**, 1083-1097 (2010).

(Received 26/10/2017;
accepted 6/12/2017)

جسيمات نانوية عالية الأداء وتأثيرها على الخواص الميكانيكية والحرارية والأشعة فوق البنفسجية لمتراكبات البولي مثيل ميثا اكريليت النانوية

هشام عبد الحى زكى مصطفى¹، نبيلة عبد الحكيم درويش¹، أحمد محمود يوسف²، سامح رضا³، عبد العزيز عرفة الوكيل¹

¹قسم متروولوجيا وتكنولوجيا البوليمرات-المعهد القومى للقياس والمعايرة - الجيزة - مصر.

²قسم مواد التعبئة والتغليف - المركز القومى للبحوث - الجيزة - مصر.

³قسم الفوتومتري والراديومتري-المعهد القومى للقياس والمعايرة - الجيزة - مصر.

الهدف من هذا العمل هو اختيار جسيمات نانوية مناسبة لتحضير متراكبات من البولي مثيل ميثا اكريلت ذات وقاية عالية من الأشعة فوق البنفسجية عند تراكيزات منخفضة وتقليل الأثار المدمرة لهذه الأشعة. تم التحقق من الأشكال المرفولوجية لهذه الجسيمات النانوية بواسطة حيود الأشعة السينية والمسح الألكترونى والمجهرى. فى حين البوليمر (PMMA) ومتراكباته النانوية قد وصيفت باستخدام التحليل الميكانيكى الديناميكي (DMA) وأختبار الشد والأشعة فوق البنفسجية والثبات الحرارى (TGA). وأظهرت النتائج التى تم الحصول عليها وجود علاقة جيدة بين خصائص الشد، والتحليل الميكانيكى الديناميكي والثبات الحرارى اعتمادا على نوع الجسيمات النانوية المستخدمة وخصوصا فى حالة أكسيد الزركونيم وأكسيد الزنك. علاوة على ذلك، تم تحليل الأشعة فوق البنفسجية فى مدى ٢٠٠ نانوميتر الى ٨٠٠ نانوميتر وأظهرت الدراسة أن الأشعة فوق البنفسجية قد حجبت بشكل كبير من ١٠٠٪ الى ٠,٢٪ بالنسبة للبوليمر (PMMA) والى ٠,٠٨٪ فى حالة المتراكب (PMMA/CeO2) والى ٠,٠١٪ للمتراكبات المضافة اليها الأنواع المختلفة من الجسيمات النانوية. بعد الطول الموجى ٣٦٠ نانوميتر، تأثر البوليمر ومتراكبه (PMMA/CeO2) قليلا بالأشعة البنفسجية فى حين لم يتأثر المتراكبات الأخرى المضاف اليها الجسيمات النانوية المختلفة. وتبين هذه النتيجة أن هذه المركبات النانوية يمكن أن تكون مرشحة بدرجة عالية للأستخدام فى المظلات الشمسية أو فى العديد من المجالات التى تتعلق بالأثار الضارة من الأشعة فوق بنفسجية .